



Scott, J.M., Liu, J., Pearson, D.G., Harris, G.A., Czertowicz, T.A., Woodland, S.J., Riches, A.J.V. and Luth, R.W. (2019) Continent stabilisation by lateral accretion of subduction zone-processed depleted mantle residues; insights from Zealandia. *Earth and Planetary Science Letters*, 507, pp. 175-186. (doi:[10.1016/j.epsl.2018.11.039](https://doi.org/10.1016/j.epsl.2018.11.039))

There may be differences between this version and the published version. You are advised to consult the publisher's version if you wish to cite from it.

<http://eprints.gla.ac.uk/174626/>

Deposited on: 05 December 2018

Enlighten – Research publications by members of the University of  
Glasgow  
<http://eprints.gla.ac.uk>

1 **Continent stabilisation by lateral accretion of**  
2 **subduction zone-processed depleted mantle residues;**  
3 **insights from Zealandia**

4 *J.M. Scott<sup>1</sup>, J. Liu<sup>2,\*</sup>, D.G. Pearson<sup>2</sup>, G.A. Harris<sup>2</sup>, T.A. Czertowicz<sup>1</sup>, S.J. Woodland<sup>2</sup>, A.J.V. Riches<sup>2\*\*</sup>,*  
5 *R.W. Luth<sup>2</sup>*

6 <sup>1</sup> Department of Geology, University of Otago, Dunedin 9054, New Zealand

7 <sup>2</sup> Department of Earth and Atmospheric Sciences, University of Alberta, Edmonton, Alberta T6G 2E3,  
8 Canada

9 \* Now at: State Key Laboratory of Geological Processes and Mineral Resources, China University of  
10 Geosciences, Beijing 100083, China

11 \*\* Now at: School of Geographical and Earth Sciences, University of Glasgow, Glasgow, G12 8QQ,  
12 United Kingdom.

13 Email: james.scott@otago.ac.nz

14 **Abstract**

15 To examine how the mantle lithosphere stabilises continents, we present a synthesis of the mantle  
16 beneath Zealandia in the SW Pacific Ocean. Zealandia, Earth's "8<sup>th</sup> continent", occurs over 4.9 M km<sup>2</sup>  
17 and comprises a fore-arc, arc and back-arc fragment rifted from the Australia-Antarctica Gondwana  
18 margin 85 Myr ago. The oldest extant crust is ~500 Ma and the majority is Permian-Jurassic. Peridotitic  
19 rocks from most known locations reveal the underpinning mantle to comprise regional domains varying  
20 from refractory ( $\text{Al}_2\text{O}_3 < 1$  wt%, olivine Mg# > 92, spinel Cr# up to 80, Pt/Ir < 1) to moderately depleted  
21 ( $\text{Al}_2\text{O}_3 = 2\text{-}4$  wt%, olivine Mg# ~90.5, spinel Cr# < ~ 60). There is no systematic distribution of these  
22 domains relative to the former arc configuration and some refractory domains underlie crust that is largely  
23 devoid of magmatic rocks. Re-depletion Os model ages have no correlation with depletion indices but do  
24 have a distribution that is very similar to global convecting mantle. Whole rock, mineral and isotopic data  
25 are interpreted to show that the Zealandia mantle lithosphere was constructed from isotopically  
26 heterogeneous convecting mantle fragments swept into the sub-arc environment, amalgamated, and  
27 variably re-melted under low-P hydrous conditions. The paucity of mafic melt volumes in most of the  
28 overlying crust that could relate to the depleted domains requires melting to have been followed by lateral  
29 accretion either during subduction or slab rollback. Recent Australia-Pacific convergence has thickened  
30 portions of the Zealandia mantle to > 160 km. Zealandia shows that the generation of refractory and/or  
31 thick continental lithosphere is not restricted to the Archean. Since Archean cratons also commonly  
32 display crust–mantle age decoupling, contain spinel peridotites with extreme Cr# numbers that require  
33 low-P hydrous melting, and often have a paucity of mafic melts relative to the extreme depletion indicated  
34 by their peridotitic roots, they too may - in part - be compilations of peridotite shallowly melted and then  
35 laterally accreted at subduction margins.

36

37 Keywords: lithosphere, peridotite, Os isotopes, continent, depleted mantle, lateral accretion, Zealandia

## 38 **1. Introduction**

39 The compositions of cratonic peridotite xenoliths have led to models in which the mantle roots to Earth's  
40 early continents formed by high-*P* melting induced by plumes (e.g., Griffin et al., 2003; Arndt et al., 2009;  
41 Aulbach, 2012), polybaric decompression melting beneath oceanic plates (e.g., Bernstein et al., 2006;  
42 Rollinson, 2010; Herzberg and Rudnick, 2012) and/or low-*P* hydrous melting in sub-arc environments  
43 (e.g., Parman et al., 2004; Pearson and Witting, 2008). The intrinsic buoyancy of depleted lithospheric  
44 peridotite compared to the convecting mantle promotes long-term lithosphere stability (e.g., Jordan,  
45 1978). The difficulty of deciphering the process of ancient lithosphere formation in part stems from the  
46 lack of consensus on when global subduction began, since subduction implies the presence of arcs, and  
47 arcs are synonymous with modern sites of hydrous melting, continent accretion and growth.

48         Whereas there are a plethora of geological, geochemical and dynamic modelling studies  
49 examining the factors leading to the stabilisation of Archean continents, relatively few focus in the same  
50 way on the role played by peridotitic lithosphere in forming Earth's younger continents. To understand the  
51 formation of young continental lithospheres, we present the results of an extensive survey, using almost  
52 all known mantle sample locations, of the composition and age of the lithospheric mantle underpinning  
53 central-southern Zealandia (**Fig. 1**). Zealandia is a 4.9 M km<sup>2</sup> Phanerozoic continent in the southwest  
54 Pacific Ocean and represents Earth's most recently stabilised continental masses (Mortimer et al., 2017).  
55 It is an ideal place to examine the formation of a continental-scale modern lithosphere because (1) it was  
56 unequivocally assembled as a result of Phanerozoic subduction along the margin of Gondwana; and (2)  
57 there are numerous exhumed fragments of its lithospheric mantle keel, in the form of ultramafic massifs  
58 and mantle xenoliths in volcanic rocks, that span the former Gondwanan Mesozoic fore-arc, arc and  
59 back-arc areas. We draw on an extensive mineral, whole rock and Os isotopic database to generate a  
60 model for how the mantle roots underpinning this young continent established and became stable. We  
61 find that Re-depletion Os model ages have little or no association with the stabilisation age, and suggest  
62 that, despite many billions of years of interim Earth evolution, there are similarities in the process of  
63 continental root assembly of Earth's youngest and oldest continents.

64

## 65 **2. Zealandia's geological context**

66 Zealandia is a largely submarine continent occurring over 4.9 million km<sup>2</sup> in the SW Pacific Ocean that  
67 comprises a near-intact fragment of the Mesozoic Gondwana arc margin (**Fig. 1**). The oldest crust is Late  
68 Cambrian and the continent is predominantly composed of younger meta-sedimentary terranes and arcs  
69 that were progressively accreted to the subduction margin throughout the Phanerozoic (**Fig. 2**) (Mortimer,

70 2004). Unlike formerly contiguous Antarctica and Australia, neither surficial nor deeply exhumed crust  
71 (e.g., Beyssac et al. 2015; Jacob et al., 2017) or zircon U–Pb–Hf isotope systematics in igneous rocks  
72 (e.g., Bolhar et al., 2008) provide evidence that Zealandia has an Archean or even Proterozoic crustal  
73 core.

74 The continental terrane assemblage of Zealandia preserves the Early Cretaceous subduction  
75 margin fore-arc, arc and back-arc configuration of Gondwana (**Fig. 2**). Subduction ceased at ~105 Ma  
76 when the Hikurangi oceanic plateau (**Fig. 2**), a significant fragment of the Ontong Java - Manihiki large  
77 igneous province, collided with the Gondwana margin. The Hikurangi Plateau was too buoyant to  
78 subduct, and this is inferred to have resulted in a shallow dipping fore-running oceanic lithosphere rolling  
79 back towards the trench and ceasing the long-lived Phanerozoic convergence (Jacob et al., 2017). This  
80 process ultimately led to the defining evolutionary stages that culminated in Zealandia's continent status:  
81 Late Cretaceous to Early Eocene development of the oceanic crust-floored Tasman Sea during  
82 separation of Zealandia from Australia, and Late Cretaceous to present day formation of oceanic crust in  
83 the Southern Ocean between Zealandia and Antarctica (e.g., Tulloch and Kimbrough, 1989; Mortimer et  
84 al., 2017).

85 The orogenic peridotites, xenoliths in alkaline basalts, and the ultramafic bases to ophiolites  
86 represent fragments of Zealandia mantle lithosphere (**Fig. 1, 2**). The Dun Mountain Ophiolite Belt – type  
87 locality of dunite – stretches for > 1000 km and represents a depleted slice of Permian oceanic  
88 lithosphere accreted in the Mesozoic (Coombs et al., 1976). The Anita Peridotite in SW New Zealand is a  
89 15 km long by up to 1 km wide refractory body that provides a snapshot of the Cretaceous sub-arc spinel  
90 facies mantle lithosphere (Czertowicz et al., 2016). The main insights into the Zealandia lithosphere,  
91 however, have come from Cretaceous to Miocene peridotite xenoliths entrained by alkaline basalts.  
92 Limited whole rock Os data (McCoy-West et al., 2013; Liu et al., 2015) and clinopyroxene Hf (Scott et al.,  
93 2014b) has revealed that peridotite suites from the West Otago and East Otago mantle domains (**Fig. 1**)  
94 contain depletion ages that span Archean to modern times. The ancient material has been interpreted to  
95 represent long-lived stable lithosphere (McCoy-West et al., 2013) or material accumulated during young  
96 lithosphere assembly (Scott et al., 2014b; Liu et al., 2015); we further address this topic in the current  
97 paper. Regardless of which model is preferred, the Zealandia mantle lithosphere records Cretaceous  
98 metasomatism by CO<sub>2</sub>-bearing silicate and carbonatitic magmas that have imparted a HIMU-like Sr-Nd-  
99 Pb ± Hf-like isotopic signature (Scott et al., 2014a, b; McCoy-West et al., 2016; Scott et al., 2016a, b;  
100 Dalton et al., 2017; van der Meer et al., 2017). Shortening across the Australia-Pacific plate boundary in  
101 the last ~7 Ma has thickened the present-day lithosphere beneath West Otago and interpretation of

102 geophysical survey results indicates that the mantle root beneath the Southern Alps now extends to >  
103 160 km (e.g., Stern et al., 2000; Sutherland et al., 2000; Reyners et al., 2017).

104

### 105 **3. Methods**

#### 106 *3.1. Whole rock geochemistry*

107 Peridotite whole rock powders were prepared by cutting samples into narrow plates and removing  
108 alteration. Sample surfaces were then cleaned with carborundum paper, washed and dried. Rocks were  
109 placed in several plastic bags and gleefully smashed with a hammer until fragments were < 1 cm.  
110 Material was then pulverised in an agate mill. A pure quartz sand was run between samples, and the mill  
111 cleaned thoroughly twice between analyses. Powders were dispatched and then processed for major and  
112 trace elements by X-ray fluorescence at Franklin & Marshall College in the United States of America or  
113 SpectraChem Analytical in New Zealand. Major elements were measured on lithium tetraborate disks  
114 containing 0.4 grams (Franklin & Marshall College) or 0.5 grams (SpectraChem Analytical) of  
115 homogenised powder. Trace elements were measured on dried powders (110°C) converted to pressed  
116 powder pellets comprising 7.0 grams of rock powder and 1.4 grams of copolywax. Elements were  
117 measured on a PANalytical 2404 X-ray fluorescence vacuum spectrometer equipped with a 4 kW Rh  
118 super sharp X-ray tube. Loss on ignition was calculated by weighing aliquots before and after being  
119 subjected to 950°C for one hour.

120

#### 121 *3.2. Os isotopes and PGE*

122 Whole rock PGE (Os, Ir, Pt, Pd and Re) concentrations and Os isotope ratios were obtained using  
123 isotope dilution at the University of Alberta. Approximately 1 gram of whole-rock powder, in combination  
124 with an appropriate amount of mixed HSE spikes ( $^{185}\text{Re}$ ,  $^{190}\text{Os}$ ,  $^{191}\text{Ir}$ ,  $^{194}\text{Pt}$ , and  $^{106}\text{Pd}$ ), was attacked by  
125 inverse Aqua Regia (3.5 ml of Teflon-distilled concentrated HCl and 6 ml of sparged Teflon-distilled  
126 concentrated  $\text{HNO}_3$ ) in a high-pressure Asher (HPA-S, Anton Paar;  $P = 130$  bar) for ~16 h at ~260°C.  
127 Osmium was extracted immediately from the acid solution by solvent extraction into  $\text{CHCl}_3$ , back  
128 extracted into HBr and further purified via micro-distillation using a  $\text{H}_2\text{SO}_4$ -dichromate solution into 15  $\mu\text{l}$   
129 of concentrated HBr. Osmium isotope ratios were measured as  $\text{OsO}_3^-$  using multiple Faraday collectors  
130 and amplifiers equipped with  $10^{12}$   $\Omega$  resistors by a Thermo Scientific Triton Plus thermal ionization mass  
131 spectrometer (TIMS) at the University of Alberta. Typical intensities of mass 240 (mainly  $^{192}\text{Os}^{16}\text{O}_3^-$ ) were  
132 0.1-0.4 V ( $10^{11}$   $\Omega$  amplifier equivalent signals; 0.001 V is equivalent to ~62500 counts per second) with  
133 50 ratios taken at 8 seconds integration per ratio. Raw ratios were first corrected for gain and baseline,

134 followed by oxygen correction using  $^{17}\text{O}/^{16}\text{O} = 0.0003749$  and  $^{18}\text{O}/^{16}\text{O} = 0.0020439$  and spike correction,  
135 and finally by instrumental mass fractionation correction using  $^{192}\text{Os}/^{188}\text{Os} = 3.083$  via the exponential  
136 law. Internal precision on  $^{187}\text{Os}/^{188}\text{Os}$  ratios was typically better than 0.05% ( $2\sigma$ ). During the analytical  
137 campaign, repeated measurements of 0.5-2.5 ng loads of Os reference materials yielded  $^{187}\text{Os}/^{188}\text{Os}$  of  
138  $0.160927 \pm 0.000173$  ( $2\sigma$ ,  $n=14$ ) for DrOsS and  $0.113796 \pm 0.000022$  ( $2\sigma$ ,  $n=10$ ) for the University of  
139 Maryland Johnson Matthey Os Standard; these ratios are within 0.01% of the accepted values.

140 HSE were separated and purified from the remaining acid solution using cation exchange column  
141 chromatography and BPHA solvent extraction. Cation exchange chromatography was implemented to  
142 reduce the concentrations of interfering elements such as Y, Cd, Rb, Zn, Cu and Ni, with BPHA solvent  
143 extraction used to remove Zr, Mo, Hf, and W. The solution remaining after Os extraction was evaporated  
144 to dryness, and the residues were dissolved in 5 ml of  $6 \text{ mol L}^{-1}$  HCl. Following this 1 ml of 30%  $\text{H}_2\text{O}_2$  was  
145 slowly added to reduce  $\text{Cr}^{\text{VI}}$  to  $\text{Cr}^{\text{III}}$ , and the solution was dried down again. The residue was dissolved in  
146 10 ml of  $0.1 \text{ mol L}^{-1}$  HCl and loaded onto the cation exchange columns (AG50W-X8, 200-400 mesh, 16  
147 mm x 240 mm column with a 50 ml reservoir). Before sample loading, the columns were cleaned with 60  
148 ml  $6 \text{ mol L}^{-1}$  HCl, and conditioned with 80 ml of  $0.1 \text{ mol L}^{-1}$  HCl. After sample loading, an additional 11 ml of  
149  $0.1 \text{ mol L}^{-1}$  HCl was eluted and collected. The resulting ~21 ml solution was then dried down and 80 ml of  
150  $6 \text{ mol L}^{-1}$  HCl was used to clean the columns. The residues were dissolved in 2 ml of  $0.5 \text{ mol L}^{-1}$  HCl and  
151 300  $\mu\text{L}$  of fresh  $0.025 \text{ mol L}^{-1}$  BPHA (Tokyo Chemical Industry: P0158-25G)  $\text{CHCl}_3$  was added to the  
152 solution, which was vigorously shaken for 5 minutes then centrifuged. The solvent extraction was  
153 completed three times, after which the 2 ml of  $0.5 \text{ mol L}^{-1}$  HCl was pipetted off and analyzed for HSE in a  
154 single cut via ICP-MS. All HSE column cuts were measured in low-resolution mode on a Nu instruments  
155 Atom at the University of Alberta. Given that the  $^{175}\text{Lu}^+$  and  $^{178}\text{Hf}^+$  signals were less than 10000 and 1000  
156 counts per second, respectively, in the sample solutions, Lu and Hf oxide isobaric interference  
157 corrections for Ir and Pt were negligible. For Pd analysis, the zirconium ( $^{90}\text{Zr}$ ) standard solution was  
158 measured to determine the oxide production rate ( $\text{ZrO}^+/\text{Zr}^+$ ) and found to be  $< 1\%$  during the analytical  
159 measurements. The isobaric interference correction of  $^{90}\text{ZrO}^+$  on mass 106 was  $< 0.1\%$ . Instrumental  
160 mass fractionation was corrected for by periodic measurements of in-house standard (GP-13; usually one  
161 per four sample analyses) using the standard bracketing method and resulted in a typically less than 1%  
162 correction.

163

## 164 **4. Results**

### 165 *4.1. Zealandia's mantle geochemistry*

166 In the context of interpreting the formation of the peridotitic root to a continent, a key feature of Zealandia  
167 is the relative abundance of mantle peridotite that has been erupted or exhumed across the Mesozoic  
168 crustal configuration of a fore-arc, arc and back-arc (**Fig.1, 2**; summarised in **Supplementary Table 1**).  
169 Although many of the rocks are variably metasomatised (McCoy-West et al., 2013; Scott et al., 2014a, b;  
170 Czertowicz et al., 2016; Scott et al., 2016a, b), bulk rock peridotite  $\text{Al}_2\text{O}_3$  concentrations show the dataset  
171 to be divisible into geographical domains that, relative to primitive upper mantle (PUM), are moderately  
172 depleted (Auckland Island, Canterbury, Dun Mountain Ophiolite Belt, East Otago) through to refractory  
173 (Anita Peridotite, Chatham Island, West Otago, Lake Moana in Westland) (**Fig. 3**; dataset summarised in  
174 **Supplementary Table 2**). The refractory domains show no systematic distribution relative to the  
175 Cretaceous arc configuration. With the exception of Auckland Island and East Otago, most of the  
176 investigated Zealandia suites are generally more depleted in incompatible major elements than abyssal  
177 peridotites, with the refractory peridotites comparable to the most depleted residues of any known age  
178 documented on Earth: fore-arc mantle, depleted ophiolite and the least metasomatised cratonic mantle  
179 compositions (e.g., Tanzanian Craton and the West and East Greenland portions of the North Atlantic  
180 Craton) (**Fig. 3**). When the refractory domain  $\text{Al}_2\text{O}_3$  compositions are compared experimental residues  
181 that have undergone 30% anhydrous melt extraction at 5, 3 and 2 GPa (Walter, 2003), the Zealandia  
182 residues plot in the realm of low- $P$  ( $< 3$  GPa) melting. Melting at higher pressure (7 GPa) stabilises garnet  
183 to very high melt extraction levels ( $\sim 50\%$ ) and effectively rules out a high- $P$  residue origin for most of  
184 these residues.

185 Like  $\text{Al}_2\text{O}_3$ , peridotite Mg# ( $100 \cdot \text{Mg}/(\text{Fe}+\text{Mg})$ ) is a well-known indicator of the degree of melt  
186 extraction. Of the refractory suites, the West Otago, Chatham Island, and Lake Moana peridotites have  
187 averaged bulk rock Mg# ranging between 90.7 and 91.8. Since it is difficult to obtain a whole rock  
188 analysis from a small xenolith, and the bulk rock analyses can be compromised by Fe-enrichment from  
189 the host melt, the composition of the most abundant peridotite mineral phase, olivine, provides more  
190 robust information with which to test the geographical extent of the Zealandia mantle domains and further  
191 assess their levels of depletion. When olivine Mg# data for 263 peridotites from 26 localities are plotted, it  
192 is evident that the moderately depleted (olivine Mg#  $\sim 90.0$ – $91.5$ ) to refractory (olivine Mg#  $\geq 91.5$  but  
193 typically 92.5) domains are regional in scale (**Fig. 4**; **Supplementary Table 4**). The high mean and  
194 median olivine Mg# of olivine from the Anita Peridotite, Lake Moana (Westland) and the Mt Alta, Lake  
195 Wanaka and MacFarlane Stream (West Otago) locations are equivalent to or only slightly less depleted  
196 than typical Archean peridotites (e.g., Bernstein et al., 2007) (**Fig. 4**). As with the bulk  $\text{Al}_2\text{O}_3$  values,



197 olivine Mg# values provide minima for melting estimates because many xenoliths have been  
198 metasomatised and experienced some Fe addition.

199 Spinel is the main host to Cr in spinel facies peridotites, and high Cr# ( $100 \cdot \text{Cr}/(\text{Cr}+\text{Al})$ ) equates to  
200 high degrees of melting in the shallow mantle (e.g., Dick and Bullen, 1984). Spinel Cr# versus olivine  
201 Mg# shows the Zealandia peridotites to span compositions from close to PUM (olivine Mg# = 89.2; spinel  
202 Cr# = 7) to forsterite-rich olivine (Mg# > 92) coexisting with chromite (Cr# > 65) equivalent to some of the  
203 most refractory spinel facies cratonic peridotite suites (**Fig. 5**). The Al-spinel and Cr-spinel-bearing East  
204 Otago and Auckland Island suites cluster at the less depleted end of the spectrum and partially overlap  
205 with the abyssal peridotite field. The Chatham Island peridotites, which come from beneath the partially  
206 subducted Hikurangi Plateau, have high olivine Mg# for their generally moderate Cr# and mostly plot at  
207 compositions that overlap the Archean peridotite field (**Fig. 5**). The Dun Mountain Ophiolite Belt  
208 peridotites plot slightly to the right of the main Zealandia trend but within the field of supra-subduction  
209 zone peridotites. The chromite-bearing Anita Peridotite, Lake Moana and West Otago samples overlap  
210 our compilations of the fields for chromite-bearing garnet-free Archean peridotites, modern supra-  
211 subduction zone peridotites, and hydrous melting experiments. A distinct feature of the olivine-spinel  
212 trends in Al-spinel to Cr-spinel-bearing rocks is that the Zealandia peridotites have lower olivine Mg# for  
213 equivalent Cr# compared to Archean xenoliths (**Fig. 5**).

#### 214 215 *4.2. Os isotope and platinum group element data*

216 Osmium isotopes and platinum group elements (PGE) have been measured in 70 peridotites from the  
217 Mesozoic back-arc (Auckland Islands, n = 8 analyses; Lake Moana, n = 9), arc (Anita Peridotite, n = 10),  
218 and from beneath the fore-arc (Chatham Island; n = 19; Dun Mountain Ophiolite Belt; n = 24). When  
219 supplemented with 5 analyses from Canterbury, 14 from East Otago, 2 from the Chatham Islands  
220 (McCoy-West et al., 2013), and 21 from West Otago (Liu et al., 2015), all from the fore-arc area, the  
221 Zealandia sample suite represents one of the largest global non-cratonic continental Os isotope and PGE  
222 datasets (**Supplementary Table 1**).

223 Zealandia peridotite Os model ages ( $T_{\text{MA}}$ ) correlate poorly with Re-depletion Os model ages ( $T_{\text{RD}}$ )  
224 in the xenoliths (**Supplementary Table 1, Fig. 1**). This is likely due to late-stage Re addition during  
225 xenolith entrainment and transport, since the  $T_{\text{MA}}$  versus  $T_{\text{RD}}$  agreement is better for the orogenic Anita  
226 Peridotite. The Os isotope compositions and their resulting  $T_{\text{RD}}$  ages indicate that the Zealandia  
227 lithospheric mantle is extremely isotopically heterogeneous.  $T_{\text{RD}}$  ages span Archean to modern times but  
228 contain the striking feature that most ages are significantly older than the Zealandia crust (**Fig. 6**). The

229 very broad  $T_{RD}$  peak centred at 1.2 Ga is analogous to that observed in the global abyssal peridotite  
230 dataset and Pt-alloys from ophiolites (e.g., Pearson et al., 2007) and quite distinct from, for example,  
231 Archean cratons (**Fig. 6**). As with bulk rock chemistries and mineral chemistries, there is no correlation  
232 between peridotite  $T_{RD}$  age and geographical distribution.

233         Aside from a subset of samples that exhibit  $Pd/Ir > PUM$ , such as those of the fore-arc Dun  
234 Mountain Ophiolite Belt and the back-arc Auckland Island peridotites, Zealandia peridotites with low  $Pd/Ir$   
235 correspond to low bulk rock  $Al_2O_3$  (**Fig. 7A**). These compositions also extend to those of cratonic  
236 peridotites, although low  $Pd/Ir$  is not necessarily indicative of Archean processes because if the PGE are  
237 mainly bound up in sulphides and alloys then  $Pd/Ir$  should not change greatly after sulphide/alloy  
238 consumption (~20-25% melting; Aulbach et al., 2016) and any refractory residue should have low  $Pd/Ir$ . A  
239 key feature of the Zealandia HSE is the broadly sub-vertical  $^{187}Os/^{188}Os$  versus  $Pd/Ir$  arrays at low  $Pd/Ir$   
240 in the most refractory suites (**Fig. 7B**). The sub-vertical Os array was first noted for Zealandia peridotites  
241 by Liu et al. (2015) in the West Otago suite but the new Chatham Islands, Lake Moana and Anita  
242 Peridotite suites data confirm this to be a continental-scale trend.

243

## 244 **5. DISCUSSION**

### 245 *5.1. Decoupling of Os isotopes and bulk rock and mineral chemistries*

246 The Zealandia peridotite  $^{187}Os/^{188}Os$  values are generally far too radiogenic to be the result of  
247 widespread Archean depletion and not radiogenic enough to represent only depletion during Paleozoic  
248 and Mesozoic crust formation. The sub-vertical Os isotope vs  $Pd/Ir$  arrays, which cannot be regressed  
249 though PUM (**Fig. 7B**), require the Zealandia peridotite Os isotopes and bulk rock chemistries to be  
250 decoupled. One interpretation of the large range in Re-depletion Os model ages (**Fig. 6**) is that the small  
251 number of Archean ages indicates that the underpinning Zealandia mantle is very old and that the Os  
252 systematics have been heavily modified by metasomatism and addition of Re. Although many Zealandia  
253 peridotites show chemical signatures of having been metasomatised (Scott et al., 2014a, b; McCoy-West  
254 et al., 2016; Scott et al., 2016a, b; Dalton et al., 2017), the lack of systematic Os versus HSE trends (**Fig.**  
255 **7A, 7B**) is inconsistent with the overall isotopic range being caused by this process. The lack of  
256 correlation between Os isotopes and depletion indices (where the lowest  $Al_2O_3$  and  $Pd/Ir$  and highest  
257 olivine Mg# samples can have either Archean or Phanerozoic model ages) belies the relationship  
258 observed in cratonic peridotites where the most depleted peridotites preserve the oldest ages (e.g.,  
259 Lugué et al., 2015). Furthermore, a long-lived mantle lithosphere scenario would require a particularly  
260 complex geodynamic model that permits a large lithospheric mantle platform to remain stable for billions

261 of years through numerous cycles of accretion of Phanerozoic oceanic crustal (**Fig. 2**) and yet  
262 experience total replacement of any Archean crust. As a measure of how likely this is, the mantle  
263 lithosphere beneath eastern Australia, immediately adjacent to the Gawler Craton, contains no vestige of  
264 Archean heritage (Handler et al., 1997).

265 An alternative explanation for the Os data is that the Zealandia lithosphere domains represent  
266 amalgamations of peridotite fragments with a spectrum of depletion ages. A key point here is that the  
267 Zealandia lithospheric mantle demonstrably contains small-scale Os isotope heterogeneities. The best  
268 example of this comes from the orogenic Anita Peridotite, for which samples within 100s of m to 1 km of  
269 one another have  $T_{RD}$  ages from 0.1-1.5 Ga (**Supplementary Fig. 2**) yet show no systematically  
270 distinguishable chemistry or mineralogy (**Figs. 5, 7**). Although this exact relationship cannot be  
271 confidently stated for the peridotite xenolith suites because they have lost their source reference frame,  
272 16 xenolith analyses from a single diatreme in West Otago yielded  $T_{RD}$  ages of 0.51-2.75 Ga but all are  
273 extremely refractory and do not define a trend that intersects PUM (Liu et al., 2015). Similar trends occur  
274 in the Chatham Island and Lake Moana datasets (**Fig. 7B**), and together the data point to lithospheric  
275 columns of Zealandia mantle containing extreme Os heterogeneity that cannot be accounted for by  
276 variable degrees of melting in a single event.

277 Abyssal and ophiolitic peridotite suites and ophiolite suite demonstrate that the convecting mantle  
278 is highly heterogeneous and also must contain small-scale Os heterogeneities (e.g., Parkinson et al.,  
279 1998; Brandon et al., 2000; Schulte et al., 2009). An important observation is that the Zealandia Os  
280 isotope range falls within the spectrum defined by abyssal peridotites (**Fig. 6**), which must globally  
281 underpin Jurassic or younger oceanic crust. Although Archean residues have not been obtained from  
282 abyssal peridotites, the removal of Archean mantle lithosphere, as well known for example in the North  
283 China Craton, requires that the convecting mantle contains some ancient components. Therefore, while  
284 there is a broad peak in the Zealandia depletion ages at 1.2 Ga, there is no evidence that this represents  
285 the “stabilisation” age of this lithosphere. In summary, three key points are: (1) the Zealandia Os model  
286 ages appear to have little or no temporal or genetic association with the overlying continental crust; (2)  
287 there is no apparent long-lived Archean-Proterozoic core to the continent, although there is no doubt that  
288 there are some ancient residues embedded within the mantle lithosphere; and (3) the Zealandia  
289 lithospheric mantle broadly preserves the inherent Os isotopic variability observed in Phanerozoic  
290 convecting mantle and is mostly likely young.

291

292 *5.2. A model for continental root formation*

293 Zealandia's oldest crustal rocks are Late Cambrian but the continent only formed as an entity free from  
294 Australia and Antarctica 85 Myr ago when the paleo-Pacific subduction margin of Gondwana fragmented  
295 and the Tasman Sea and Southern Ocean opened (**Fig. 1**). Any model for the formation and stabilisation  
296 of the Zealandia lithosphere needs to address how Phanerozoic continental crust can be underlain by a  
297 mantle lithosphere containing regional domains that: (1) vary from moderately depleted to highly  
298 refractory, (2) commonly have  $T_{RD}$  ages decoupled from PGE systematics and major element  
299 compositions, and (3) have histories extending to billions of years before crust formation. We propose  
300 that these three features can be explained by the lithospheric mantle having been constructed from  
301 mixing of an array of heterogeneous peridotite fragments swept together beneath the Gondwana  
302 subduction margin, variably re-melted, and then laterally accreted.

303 In our model, the refractory peridotite domains represent previously depleted mantle with minimal  
304 remaining Re – and hence unradiogenic Os – that underwent re-melting in some cases to generate the  
305 extremely low  $Al_2O_3$ , high olivine Mg# and high spinel Cr# harzburgitic to dunitic residues (**Fig. 8A**). It is  
306 very unlikely that the highly refractory parts of this lithosphere could have been produced *in situ* by, for  
307 instance, plume residue accretion. This is because there is no geological or geophysical evidence for the  
308 presence of plume-related magmatic rocks anywhere in the Zealandia crust except for the Hikurangi  
309 Plateau in the northeast (**Fig. 1, 2**) and because there is a clear crust-mantle age decoupling in most  
310 areas (**Fig. 6**). The high olivine Mg# in the most depleted Zealandia peridotite suites requires  $\geq 30\%$  melt  
311 extraction, which is the point of orthopyroxene exhaustion (Bernstein et al., 2006, 2007). These levels of  
312 depletion, coupled with the low bulk  $Al_2O_3$  (**Fig. 3**) and the very high spinel Cr# have been shown to be  
313 achievable only via low-P melting of peridotite in the presence of modest amounts of water (e.g., Mitchell  
314 and Grove, 2015; **Supplementary Table 5**). Peridotites with low  $Al_2O_3$  and high olivine Mg# and spinel  
315 Cr# occur in modern arc lithospheres, as indicated, for example, in the SW Pacific Ocean by the  
316 widespread occurrence of young boninitic arc magmas (Crawford, 1989), depleted peridotite from mantle  
317 lithosphere such as the Mariana arc (Parkinson et al., 1992), and refractory mantle associated with  
318 ophiolite belts such as exemplified by Papua New Guinea (Jaques et al., 1980; Kaczmarek et al., 2015),  
319 and, to a lesser degree, the Dun Mountain Ophiolite belt (**Fig. 3**).

320 The low-P hydrous melting of already Re-depleted peridotite may have occurred along the  
321 Gondwana subduction margin in the part of the asthenospheric mantle wedge influence by corner flow,  
322 as has been invoked to explain the refractory residues at the Mariana trench (e.g., Parkinson et al.,  
323 1998), which have Os model ages and bulk compositions similar to the range of the Zealandia  
324 peridotites. Mantle residues may be trapped by corner-flow and extensively flux melted by fluid sourced

325 from dehydration of serpentinite that forms above the subducting slab, giving rise to even more refractory  
326 compositions. On the other hand, the moderately depleted mantle lithospheric domains such as beneath  
327 the Auckland Islands, East Otago, and Canterbury, may represent oceanic peridotite that was brought to  
328 the subduction margin but not subjected to high degrees of sub-arc hydrous re-melting, thus explaining  
329 their mildly depleted bulk compositions (**Fig. 3**) with spinel-olivine relations that closely mirror the abyssal  
330 peridotite trend (**Fig. 5**). In the Zealandia example, one exception for arc-melting may be the depleted  
331 Chatham Island xenoliths. These originate from beneath the Hikurangi Plateau and by comparison with  
332 peridotites erupted through the once contiguous Ontong Java Plateau (Ishikawa et al., 2011) could  
333 represent portions of oceanic mantle that re-melted during Early Cretaceous plume interaction (**Fig. 8B**).

334         Progressive lateral accretion of variably aged and depleted mantle fragments during the  
335 Phanerozoic assembly of Zealandia generated a sub-continental lithospheric mantle comprising domains  
336 that do not relate genetically to the overlying crust (**Fig. 8B**). This result is exemplified by the refractory  
337 West Otago mantle domain that underpins a thick meta-sedimentary crustal pile that is almost devoid of  
338 igneous rocks as indicated by exposures of lower crustal rock exhumed along the Alpine Fault (e.g.,  
339 Beyssac et al., (2016) or as crustal xenoliths (e.g., Jacob et al., 2017). However, even the moderately  
340 depleted East Otago and Canterbury domains (e.g., **Fig. 4**) are overlain by crust that contains minimal  
341 magmatic rocks. Subduction margins provide an excellent site for the lateral accretion of mantle  
342 lithosphere, since these are prime sites of separation of crust from mantle during subduction, or  
343 extensive lateral modification during slab-rollback events. A consequence of the observations and model  
344 is that any oceanic crust accreted along with the lithosphere must have been removed by density settling  
345 during eclogite-formation (e.g. Percival and Pysklywec, 2007; Lee et al. 2011), which is consistent with  
346 the absence of eclogite xenoliths in the Zealandia mantle suites. We conclude that the widespread  
347 occurrence of refractory residues in the Zealandia mantle has led to a continental root that is more  
348 depleted and therefore more buoyant than the convecting mantle and this resulted in stabilisation of this  
349 continental mass.

350         Zealandia is not the only stable post-Archean continental area to be underlain by an array of  
351 complex and variably depleted residues with histories distinct from the overlying crust. Another example  
352 comes from peridotite xenoliths from Patagonia and southern Argentina, which have moderately depleted  
353 to refractory compositions with Os isotope compositions that broadly mimic the convecting mantle, have  
354 little or no correlation with bulk rock depletion indices, and are age-distinct from the overlying crust (e.g.,  
355 Schilling et al., 2008; Mundl et al., 2016). While the spread in Os isotope compositions are argued to  
356 have been affected by melt percolation (Mundl et al., 2016), an alternate view, by analogy with Zealandia,

357 could be that the southern South America lithospheric mantle is younger than thought and composed of  
358 heterogeneous residues compiled at the Gondwanan subduction margin and then laterally displaced from  
359 their melt locations. The moderate to refractory lithospheric mantle beneath southeast Australia (e.g.,  
360 Handler et al., 1997), Antarctica (Handler et al., 2003) and the Canadian Cordillera (e.g., Peslier et al.,  
361 2000), all located on Paleozoic and Mesozoic subduction margins, also have late Proterozoic Os model  
362 ages older than their known overlying crust. Either lateral accretion has played a key role in juxtaposing  
363 crust and mantle, and/or the underlying mantle records the Os isotope history of the convecting mantle at  
364 the time of stabilisation. In either case, the data re-enforce the conclusions (1) that peridotite Os age data  
365 in some post-Archean continental areas may have little significance in defining the “stabilisation” of  
366 lithosphere, and (2) subduction margins play a fundamental role in accumulating and accreting mantle  
367 residues.

368

### 369 *5.3. Implications for the formation of ancient continents*

370 Should the Zealandia lithosphere thicken, it would develop a garnet-bearing peridotite keel that would in  
371 many places be compositionally similar to common Archean mantle lithosphere but with much younger  
372 Re-depletion Os model ages (**Fig. 8C**). Upon becoming thickened, the high-Cr spinels in the Zealandia  
373 lithosphere should react with orthopyroxene to make high-Cr low-Ca garnets of the type documented in  
374 many Archean peridotite suites and proposed to originate by metamorphism of lower pressure chromite-  
375 bearing peridotites (e.g., Brey and Shu, 2018). In fact, crust and mantle lithospheric thickening due to  
376 plate boundary convergence has already occurred beneath the western portion of the South Island in  
377 New Zealand adjacent to the Australia-Pacific plate boundary in the last ~7 Ma. From seismic detection  
378 of a high-velocity zone beneath the Southern Alps, the mantle lithosphere there is now interpreted to  
379 extend to > 160 km depth in some places (e.g., Stern et al., 2000; Sutherland et al., 2000).

380 The cause of the thickened Zealandia lithosphere remains debated, being attributed to a west-  
381 dipping subducted slab (Sutherland et al., 2000), an east-dipping subducted oceanic plateau (Reyners et  
382 al., 2017) or plate boundary contraction (Stern et al., 2000). Regardless of which model is preferred,  
383 since the Miocene-wide southern Zealandia lithosphere was only 70-80 km thick (Scott et al., 2014a, b),  
384 this means that the West Otago refractory mantle that was sampled ~25 Myr ago from beneath the future  
385 Southern Alps prior to thickening occurred, has now likely been displaced to greater depths. Sampling of  
386 a present-day root beneath the Southern Alps, or a putatively continent-wide thickened Zealandia mantle  
387 lithosphere, would reveal the presence of a mixture of moderately depleted to refractory subduction zone  
388 residues along with plume residues from beneath the Hikurangi Plateau broadly resembling Archean

389 cratonic mantles compositions. A difference would be that Archean cratonic mantle residues would  
390 include higher degrees of depletion due to the higher ambient mantle potential temperature. The  
391 Zealandia mantle composition therefore reinforces the concept that generation of refractory mantle  
392 residues and extreme thickening of lithosphere is not restricted to Archean processes. The seismically  
393 imaged mantle beneath the Tibetan Plateau has been interpreted as an analogue for Archean cratonic  
394 mantle formation via tectonic thickening (McKenzie and Priestley, 2016). Although pre-Miocene mantle  
395 there was sampled by basaltic volcanism, the lack of very recent deep-seated volcanism penetrating this  
396 actively forming 200 km-thick root means that refractory mantle – if present – has yet to be documented.

397 Peridotite melting calculations (e.g., Canil, 2004; Lee and Chin, 2014), geochemical parameters  
398 (e.g., Pearson and Wittig, 2008) and the occurrence of high-Cr low Ca garnets in cratonic peridotites  
399 (e.g., Brey and Shu, 2018) also indicate that Archean cratonic mantle lithospheres may have formed at  
400 low-P and were thickened to great depths. The near-invariant olivine composition versus wide-ranging  
401 spinel Cr# in Archean garnet-free peridotites is, however, distinct from the over-arching Zealandia trend  
402 at the low Cr# end (**Fig. 5**). This Archean trend has been interpreted to represent polybaric anhydrous  
403 melting (Bernstein et al. 2006, 2007) but experimental data on anhydrous melting of typical mantle  
404 compositions indicate that the highest residual spinel Cr# possible by this mechanism is only ~ 60  
405 (**Supplementary Figures 3-4**).

406 While the low spinel Cr# at high olivine Mg# trend of cratonic peridotites defined in **Fig. 5** may be  
407 generated by other processes compared to more modern refractory residues (e.g., Archean spinel  
408 compositions could represent melting first in the garnet field to obtain high Mg# (in olivine) but retain Cr  
409 (in garnet), followed by decompression and re-equilibration in the spinel facies accompanied by hydrous  
410 melting to shift refractory bulk compositions to lower Al/Cr), the only experimentally determined method  
411 for formation of chromite compositions in peridotite at mantle conditions involves wet melting. For  
412 example, spinel Cr# of ~70 to 80 coexisting with olivine Mg# > 92 has been experimentally attained at ~  
413 40% melting at < 2 GPa (e.g., Hirose and Kawamoto, 1995; Mitchell and Grove, 2015; **Supplementary**  
414 **Figures 5-6**). The formation of garnet-free Archean peridotites with high Cr-spinel/chromite could  
415 therefore share a melting stage with the most depleted subduction-modified residues beneath Zealandia  
416 – that is, via melt extraction at low-P in a hydrous sub-arc environment. Moreover, like Zealandia,  
417 Archean cratons commonly comprise an amalgamation of distinct crustal blocks representing juxtaposed  
418 terranes distributed with remarkable similarity to terranes accreted at Phanerozoic subduction margins  
419 (e.g., the Superior Craton; Percival et al., 2006).

420 A feature of Zealandia is the decoupling of mantle depletion ages and the overlying crust age,  
421 and such decoupling is also hinted at in Archean cratons. Global compilations of Os isotope Re-depletion  
422 ages and U-Pb zircon data indicate that there is a general coupling of melting events in the crust and  
423 mantle (Pearson et al., 2007; Pearson and Wittig, 2008; Lee et al., 2011); however, Meso- to Eoarchean  
424 crustal units that occur in most cratons do not correlate with mantle melting events. In addition, Archean  
425 crustal rocks have a distinct scarcity in komatiite and basalt compared to the widespread abundance of  
426 underlying refractory residues (e.g., Parman et al., 2004). By analogy with Zealandia, these features may  
427 be explained by the cratonic mantle having undergone high levels of depletion – potentially by a variety of  
428 mechanisms in different tectonic settings but likely including wet melting at low-P – before being laterally  
429 displaced from the melting. The result of re-melting of such refractory mantle lithosphere would be  
430 boninite-equivalent high-MgO rocks, which is consistent with some occurrences in cratons (e.g., Polat et  
431 al., 2001; Parman et al., 2004). Subsequent thickening of the Archean root by convergence will then  
432 displace the residues to great depth and lead to garnet-bearing refractory peridotite lithosphere (e.g.,  
433 Jordan, 1978; McKenzie and Priestley, 2016; Wang et al., 2018). By analogy with the formation of Earth's  
434 youngest continent, subduction margins would be prime locations for this series of processes to have  
435 occurred to stabilise ancient continents.

436

## 437 **6. Conclusions**

438 Examination of mantle peridotites from many locations across Zealandia, a Late Cretaceous rifted  
439 fragment of the Gondwana margin and Earth's most recently stabilised continent, reveals that it is  
440 underlain by a compositionally and isotopically heterogeneous mantle lithosphere. There is no systematic  
441 distribution to moderately depleted to refractory domains. Re-depletion Os isotope model ages, which are  
442 extremely variable within individual sample suites and do not correlate with depletion indices, give dates  
443 that range as far back as Archean but have a broad peak at ~ 1.2 Ga similar to the modern convecting  
444 mantle. The Zealandia mantle lithosphere is interpreted to have been constructed from isotopically  
445 heterogeneous oceanic mantle fragments swept into the Gondwana sub-arc environment, compiled,  
446 variably re-melted under hydrous conditions at low-P to generate the refractory residues, and then  
447 laterally accreted to displace the residues from the melting location. Subsequent thickening associated  
448 with the present-day Australia-Pacific plate boundary has displaced portions of the lithospheric mantle to  
449 > 160 km (e.g., cratonic depths). This example, and that of the Himalaya, indicates that the formation of  
450 depleted residues and displacement to near craton-equivalent depths is not restricted to Archean times.  
451 Some Archean cratonic peridotites also have extreme spinel Cr# that appear to be only achievable by



452 hydrous melting, whereas others possess high-Cr garnet that could have formed via metamorphism at  
453 elevated P of high Cr-bearing spinel. Because the Archean crust often lacks sufficient mafic melts to  
454 explain the extremely depleted peridotitic roots, Archean lithospheric mantle may also be accumulations  
455 of variably depleted peridotite that was re-melted at a subduction margin to give high spinel Cr# and  
456 olivine Mg#, laterally accreted, and then thickened to high-P to form garnet. The stabilisation of the root  
457 to Earth's old continents may therefore have formation processes in common with Earth's youngest  
458 continents.

459

#### 460 **Acknowledgements**

461 Sample collection and analysis was largely funded by a New Zealand Foundation for Research Science  
462 and Technology and University of Otago Research grants to JMS and a Canada Excellence Research  
463 Chairs program to DGP. Some Dun Mountain Ophiolite Belt fieldwork was supported by National  
464 Geographic Waitt Foundation grant 2841-3 to AJVR. Emily Chin and Roberta Rudnick are thanked for  
465 reviewing the text.

466

#### 467 **References**

- 468 1. Arndt, N.T., Coltice, N., Helmstaedt, H. Gregoire, M. 2009. Origin of Archean subcontinental  
469 lithospheric mantle: Some petrological constraints. *Lithos* 109, 61-71.
- 470 2. Aulbach, S. 2012. Craton nucleation and formation of thick lithospheric roots. *Lithos*, 149, 16-30.
- 471 3. Aulbach, S., Mungall, J.E. Pearson, D.G. 2016. Distribution and processing of highly siderophile  
472 elements in cratonic mantle lithosphere. *Rev. Mineral. Geochem.* 81, 239-304.
- 473 4. Bernstein, S., Kelemen, P.B., Hanghøj, K. 2007. Consistent olivine Mg# in cratonic mantle  
474 reflects Archean mantle melting to the exhaustion of orthopyroxene. *Geology* 35, 459-462.
- 475 5. Bernstein, S., Hanghøj, K., Kelemen, P.B., Brooks, C.K. 2006. Ultra-depleted, shallow cratonic  
476 mantle beneath West Greenland: dunitic xenoliths from Ubekendt Ejland. *Con. Min. Pet.* 152,  
477 335-347.
- 478 6. Beyssac, O., Cox, S.C., Vry, J., Herman, F. 2016. Peak metamorphic temperature and thermal  
479 history of the Southern Alps (New Zealand). *Tectonophysics*, 676, 229-249.
- 480 7. Bolhar, R. Weaver, S.D., Whitehouse, M.J., Palin, J.M., Woodhead, J.D. Cole, J.W. 2008.  
481 Sources and evolution of arc magmas inferred from coupled O and Hf isotope systematics of  
482 plutonic zircons from the Cretaceous Separation Point Suite (New Zealand). *Earth Planet. Sci.*  
483 *Lett.* 268, 312-324.

- 484 8. Brandon, A.D., Snow, J.E., Walker, R.J., Morgan, J.W. and Mock, T.D., 2000.  $^{190}\text{Pt}$ – $^{186}\text{Os}$  and  
485  $^{187}\text{Re}$ – $^{187}\text{Os}$  systematics of abyssal peridotites. *Earth Planet. Sci. Lett.* 177, 319-335.
- 486 9. Brey, G.P., Shu, Q. 2018. The birth, growth and ageing of the Kaapvaal subcratonic mantle. *Min.*  
487 *Pet.*, in press.
- 488 10. Canil, D. 2004. Mildly incompatible elements in peridotites and the origins of mantle lithosphere.  
489 *Lithos* 77, 375-393.
- 490 11. Crawford A.J., Falloon T.J., Green, D.H., 1989. Classification, petrogenesis and tectonic setting  
491 of boninites. In: *Boninites and Related Rocks*, edited by A. J. Crawford, Unwin, London, 1-49.
- 492 12. Coombs, D.S., Landis, C.A., Norris, R.J., Sinton, J.M., Borns, D.J., Craw, D. 1976. The Dun  
493 Mountain ophiolite belt, New Zealand, its tectonic setting, constitution, and origin, with special  
494 reference to the southern portion. *Am. J. Sci.* 276, 561-603.
- 495 13. Czertowicz, T.A., Scott, J.M., Waight, T.E., Palin, J.M., van der Meer, Q.H.A., Le Roux, P.,  
496 Münker, C. Piazzolo, S. 2016. The Anita Peridotite, New Zealand: Ultra-depletion and subtle  
497 enrichment in the sub-arc mantle. *J. Petrol.* 57, 717–750.
- 498 14. Dalton, H.B., Scott, J.M., Liu, J., Waight, T.E., Pearson, D.G., Brenna, M., Le Roux, P. Palin,  
499 J.M., 2017. Diffusion-zoned pyroxenes in an isotopically heterogeneous mantle lithosphere  
500 beneath the Dunedin Volcanic Group, New Zealand, and their implications for intraplate alkaline  
501 magma sources. *Lithosphere* 9, 463-475.
- 502 15. Dick, H.J., Bullen, T. 1984. Chromian spinel as a petrogenetic indicator in abyssal and alpine-  
503 type peridotites and spatially associated lavas. *Con. Min. Pet.* 86, 54-76.
- 504 16. Griffin, W.L. O'Reilly, S.Y., Abe, N., Aulbach, S., Davies, R.M., Pearson, N.J., Doyle, B.J., Kivi, K.  
505 2003. The origin and evolution of Archean lithospheric mantle. *Precam. Res.* 127, 19-41.
- 506 17. Handler, M.R., Bennett, V.C., Esat, T.M. 1997. The persistence of off-cratonic lithospheric  
507 mantle: Os isotopic systematics of variably metasomatised southeast Australian xenoliths. *Earth*  
508 *Plan. Sci. Lett.* 151, 61-75.
- 509 18. Herzberg, C., Rudnick, R. 2012. Formation of cratonic lithosphere: an integrated thermal and  
510 petrological model. *Lithos* 149, 4-15.
- 511 19. Hirose, K., Kawamoto, T. 1995. Hydrous partial melting of lherzolite at 1 GPa: the effect of H<sub>2</sub>O  
512 on the genesis of basaltic magmas. *Earth Planet. Sci. Lett.* 133, 463-473.
- 513 20. Ishikawa, A., Pearson, D.G., Dale, C.W. 2011. Ancient Os isotope signatures from the Ontong  
514 Java Plateau lithosphere: Tracing lithospheric accretion history. *Earth Planet. Sci. Lett.*, 301, 159-  
515 170.

- 516 21. Jacob, J.-B., Scott, J.M., Turnbull, R.E., Tarling, M.S., Sagar, M.W. 2017. High- to  
517 ultrahigh- temperature metamorphism in the lower crust: An example resulting from Hikurangi  
518 Plateau collision and slab rollback in New Zealand. *J. Met. Geol.* 35, 831-853.
- 519 22. Jaques, A.L. Chappell, B.W. 1980. Petrology and trace element geochemistry of the Papuan  
520 ultramafic belt. *Con. Min. Pet.* 75, 55-70.
- 521 23. Jordan, T.H. 1978. Composition and development of the continental tectosphere. *Nature* 274,  
522 544-548.
- 523 24. Kaczmarek, M.A., Jonda, L., Davies, H.L. 2015. Evidence of melting, melt percolation and  
524 deformation in a supra-subduction zone (Marum ophiolite complex, Papua New Guinea). *Con.*  
525 *Min. Pet.* 170, 19p.
- 526 25. Lee, C.-T. A., Chin, E.J. 2014. Calculating melting temperatures and pressures of peridotite  
527 protoliths: Implications for the origin of cratonic mantle. *Earth Planet. Sci. Lett.* 403, 273-286.
- 528 26. Lee, C.-T. A., Luffi, P., Chin, E.J. 2011. Building and destroying continental mantle. *An. Rev.*  
529 *Earth Planet. Sci.*, 39, 59-90.
- 530 27. Liu, J., Scott, J.M., Martin, C.E. Pearson, D.G. 2015. The longevity of Archean mantle residues in  
531 the convecting upper mantle and their role in young continent formation: *Earth Planet. Sci. Lett.*  
532 424, 109–118.
- 533 28. Luguet, A., Behrens, M., Pearson, D. G., König, S., Herwartz, D. 2015. Significance of the whole  
534 rock Re–Os ages in cryptically and modally metasomatised cratonic peridotites: Constraints from  
535 HSE–Se–Te systematics. *Geochim. Cosmo. Acta* 164, 441-463.
- 536 29. McCoy-West, A.J., Bennett, V.C., Amelin, Y. 2016. Rapid Cenozoic ingrowth of isotopic  
537 signatures simulating “HIMU” in ancient lithospheric mantle: Distinguishing source from process.  
538 *Geochim. Cosmo. Acta* 187, 79-101.
- 539 30. McCoy-West, A.J., Bennett, V.C., Puchtel, I.S., Walker, R.J. 2013. Extreme persistence of  
540 cratonic lithosphere in the southwest Pacific: Paleoproterozoic Os isotopic signatures in  
541 Zealandia. *Geology* 41, 231–234 .
- 542 31. McKenzie, D., Priestley, K. 2016. Speculations on the formation of cratons and cratonic basins.  
543 *Earth Planet. Sci. Lett.* 435, 94-104.
- 544 32. Meisel, T., Walker, R.J., Irving, A.J., Lorand, J.P., 2001. Osmium isotopic compositions of mantle  
545 xenoliths: a global perspective. *Geochim. Cosmo. Acta*, 65, 1311-1323.
- 546 33. Mitchell, A.L., Grove, T.L. 2015. Melting the hydrous, subarc mantle: the origin of primitive  
547 andesites. *Con. Min. Pet.* 170, 23p.

- 548 34. Mortimer, N. 2004. New Zealand's geological foundations. *Gondwana Res.*, 7, 261-272.
- 549 35. Mortimer, N. Campbell, H.J., Tulloch, A.J., King, P.R., Stagpoole, V.M., Wood, R.A., Rattenbury,  
550 M.S., Sutherland, R., Adams, C.J., Collot, J. Seton, M. 2017. Zealandia: Earth's hidden continent.  
551 *GSA Today* 27, 27-35.
- 552 36. Mundl, A., Ntaflos, T., Ackerman, L., Bizimis, M., Bjerg, E.A., Wegner, W., Hauzenberger, C.A.  
553 (2015). Geochemical and Os–Hf–Nd–Sr isotopic characterization of north Patagonian mantle  
554 xenoliths: implications for extensive melt extraction and percolation processes. *J. Pet.* 57, 685-  
555 715.
- 556 37. Parkinson, I.J., Hawkesworth, C.J. Cohen, A.S. 1998. Ancient mantle in a modern arc: Osmium  
557 isotopes in Izu-Bonin-Mariana forearc peridotites. *Science* 281, 2011-2013.
- 558 38. Parman, S.W., Grove, T.L., Dann, J.C. De Wit, M.J. 2004. A subduction origin for komatiites and  
559 cratonic lithospheric mantle. *South Af. J. Geol.* 107, 107-118.
- 560 39. Pearson, D.G., Wittig, N. 2008. Formation of Archaean continental lithosphere and its diamonds:  
561 the root of the problem. *J. Geol. Soc., London* 165, 895-914.
- 562 40. Pearson, D.G., Parman, S.W. Nowell, G.M. 2007. A link between large mantle melting events  
563 and continent growth seen in osmium isotopes. *Nature* 449, 202–205.
- 564 41. Pearson, D.G., Carlson, R.W., Shirey, S.B., Boyd, F.R., Nixon, P.H. 1995. Stabilisation of  
565 Archaean lithospheric mantle: A Re-Os isotope study of peridotite xenoliths from the Kaapvaal  
566 craton. *Earth Planet. Sci. Lett.* 134, 341-357
- 567 42. Percival, J.A., Pysklywec, R.N. 2007. Are Archean lithospheric keels inverted? *Earth*  
568 *Planet. Sci. Lett.* 254, 393-403.
- 569 43. Percival, J.A., Sanborn-Barrie, M., Skulski, T., Stott, G.M., Helmstaedt, H., White, D.J. 2006.  
570 Tectonic evolution of the western Superior Province from NATMAP and Lithoprobe studies. *Can.*  
571 *J. Earth Sci.* 43, 1085-1117.
- 572 44. Peslier, A.H., Reisberg, L., Ludden, J., Francis, D. 2000. Os isotopic systematics in mantle  
573 xenoliths; age constraints on the Canadian Cordillera lithosphere. *Chem. Geol.* 166, 85-101.
- 574 45. Polat, A., Hofmann, A.W., Rosing, M.T. 2002. Boninite-like volcanic rocks in the 3.7–3.8 Ga Isua  
575 greenstone belt, West Greenland: geochemical evidence for intra-oceanic subduction zone  
576 processes in the early Earth. *Chem. Geol.* 184, 231-254.
- 577 46. Reyners, M., Eberhart-Phillips, D., Upton, P., Gubbins, D. 2017. Three-dimensional imaging of  
578 impact of a large igneous province with a subduction zone. *Earth Planet. Sci. Lett.* 460, 143-151.

- 579 47. Rollinson, H. 2010. Coupled evolution of Archean continental crust and subcontinental  
580 lithospheric mantle. *Geology*, 38, 1083-1086.
- 581 48. Schilling, M.E., Carlson, R.W., Conceição, R.V., Dantas, C., Bertotto, G.W., Koester, E. 2008.  
582 Re–Os isotope constraints on subcontinental lithospheric mantle evolution of southern South  
583 America. *Earth Planet. Sci. Lett.*, 268, 89-101.
- 584 49. Schulte, R.F., Schilling, M., Anma, R., Farquhar, J., Horan, M.F., Komiya, T., Piccoli, P.M.,  
585 Pitcher, L., Walker, R.J., 2009. Chemical and chronologic complexity in the convecting upper  
586 mantle: Evidence from the Taitao ophiolite, southern Chile. *Geochim. Cosmo. Acta* 73, 5793-  
587 5819.
- 588 50. Scott, J.M., Liu, J., Pearson, D.G., Waight, T.E. 2016a. Mantle depletion and metasomatism  
589 recorded in orthopyroxene in highly depleted peridotites. *Chem. Geol.* 441, 280-291.
- 590 51. Scott, J.M., Hodgkinson, A., Palin, J.M., Waight, T.E., van der Meer, Q.H.A., Cooper, A.F. 2014a.  
591 Ancient melt depletion overprinted by young carbonatitic metasomatism in the New Zealand  
592 lithospheric mantle. *Con. Min. Pet.* 167, 963.
- 593 52. Scott, J.M., Waight, T.E., van der Meer, Q.H.A., Palin, J.M., Cooper, A.F., Münker, C. 2014b.  
594 Metasomatized ancient lithospheric mantle beneath the young Zealandia microcontinent and its  
595 role in HIMU- like intraplate magmatism. *Geochem. Geophys. Geosys.* 15, 3477-3501
- 596 53. Scott, J.M., Brenna, M., Crase, J.A., Waight, T.E., van der Meer, Q.H., Cooper, A.F., Michael  
597 Palin, J., Le Roux, P., Münker, C., 2016b. Peridotitic lithosphere metasomatized by volatile-  
598 bearing melts, and its association with intraplate alkaline HIMU-like magmatism. *J. Petrol.* 57,  
599 2053-2078.
- 600 54. Stern, T., Molnar, P., Okaya, D., Eberhart- Phillips, D. 2000. Teleseismic P wave delays and  
601 modes of shortening the mantle lithosphere beneath South Island, New Zealand. *J. Geophys.*  
602 *Res.: Solid Earth* 105, 21615-21631.
- 603 55. Sutherland, R., Davey, F., Beavan, J. 2000. Plate boundary deformation in South Island, New  
604 Zealand, is related to inherited lithospheric structure. *Earth Planet. Sci. Lett.* 177, 141-151.
- 605 56. Tulloch, A. J., & Kimbrough, D. L. (1989). The Paparoa metamorphic core complex, New  
606 Zealand: Cretaceous extension associated with fragmentation of the Pacific margin of  
607 Gondwana. *Tectonics*, 8, 1217-1234.
- 608 57. van der Meer, Q.H.A., Waight, T.E., Scott, J.M., Münker, C. 2017. Variable sources for  
609 Cretaceous to recent HIMU and HIMU-like intraplate magmatism in New Zealand. *Earth Planet.*  
610 *Sci. Lett.* 469, 27-41.

- 611 58. Walter, M.J. 2003. Melt extraction and compositional variability in mantle lithosphere. In: Holland,  
612 H. D., Turekian, K. K. (Eds.), Treatise on Geochemistry, 1st ed. Elsevier, Oxford, pp. 363–392.
- 613 59. Wang, H., van Hunen, J., Pearson D.G. Making Archean cratonic roots by lateral compression.  
614 Tectonophys, in press. <https://doi.org/10.1016/j.tecto.2016.12.001>
- 615 60. Wittig, N. Pearson, D.G., Webb, M., Ottley, C.J., Irvine, G.J., Kopylova, M., Jensen, S.M., Nowell,  
616 G.M. 2008. Origin of cratonic lithospheric mantle roots: A geochemical study of peridotites from  
617 the North Atlantic Craton, West Greenland. Earth Planet. Sci. Lett. 274, 24-33.

618

619 **Figure 1.** Make-up of the 4.9 M km<sup>2</sup> continent of Zealandia in the SW Pacific Ocean. This continent, of  
620 which the islands of New Zealand form ~ 6 % by area above water, represents a rifted portion of the fore-  
621 arc, arc and back arc to the Australia–Antarctica–New Zealand Mesozoic subduction margin of  
622 Gondwana (inset). Mesozoic fore-arc mantle is represented by xenoliths in Cretaceous–Cenozoic basalts  
623 in Canterbury, Chatham Island, East Otago, and West Otago, as well as along the > 2000 km long  
624 Permian Dun Mountain Ophiolite Belt. Arc mantle is represented by the orogenic Anita Peridotite. Back-  
625 arc mantle was sampled by Cretaceous and Miocene basalts at Lake Moana in Westland and on  
626 Auckland Island, respectively. The size of the stars indicates the extent of the different peridotite suites.

627

628 **Figure 2.** Zealandia is composed of an array of accreted terranes, here shown according to their  
629 Cretaceous back-arc, arc and fore-arc positions. Terrane relative ages and main compositions are  
630 indicated on the lower diagram. Terrane information is taken from the summary provided in Mortimer  
631 (2004).

632

633 **Figure 3.** Box and whisker plots of peridotite bulk rock Al<sub>2</sub>O<sub>3</sub>, normalised to 100 wt.% anhydrous. These  
634 data illustrate the heterogeneity in the Zealandia lithospheric mantle and show that the refractory  
635 Zealandia peridotites are comparable to depleted fore-arc (Marianna Arc, Kamchatka Arc), depleted  
636 ophiolite (Luobusa, Papua New Guinea) and least metasomatised cratonic mantle (North Atlantic Craton,  
637 Tanzania Craton and the Murowa location in the Zimbabwe Craton). Comparison of the refractory  
638 Zealandia peridotites (Westland, Anita, West Otago) with experimentally determined Al<sub>2</sub>O<sub>3</sub> contents of a  
639 residue after 30 % partial melting at 5, 3 and 2 GPa (Al<sub>2</sub>O<sub>3</sub> concentrations from the experiments of  
640 Walter, 2003) implies that they reached their low Al<sub>2</sub>O<sub>3</sub> contents at P ≤ 3 GPa. PUM is from Meisel et al.  
641 (2001). Data sources for suites are in **Supplementary Tables 2 and 3.**

642

643 **Figure 4.** Summary of olivine Mg# data for 263 Zealandia peridotites. Boxes show the median values  
644 and the 1<sup>st</sup> and 3<sup>rd</sup> quartiles for each dataset. Some Zealandia samples have experienced Fe addition  
645 that has lowered their olivine Mg#, such as from the Burke River and Moeraki locations in West Otago  
646 and Cape L'Evique and Ohira Bay from Chatham Island (see Scott et al., 2014a, b, 2016a, b for  
647 discussion), and Hohonu Westland suite. Data are summarised in **Supplementary Tables 4** and **6**.  
648 Average Archean cratonic compositions are from the compilations of Bernstein et al. (2006, 2007) and  
649 Pearson & Wittig (2008).

650

651 **Figure 5.** Spinel Cr# versus olivine Mg# for the Zealandia peridotites compared to global fields of abyssal  
652 peridotite, supra-subduction zone peridotite, Archean peridotites and the results of peridotite anhydrous  
653 and hydrous melting experiments. The Supplementary File provides references for these large datasets,  
654 and an up-to-date compilation of Archean spinel facies peridotites and experimental melting  
655 compositions. The orthopyroxene-out and clinopyroxene-out for low-P melting are estimated from  
656 Bernstein et al. (2006, 2007) and Scott et al. (2016b), respectively.

657

658 **Figure 6.** Summary of whole rock Re-depletion Os model ages for Zealandia (McCoy-West et al., 2013;  
659 Liu et al., 2015; this study). The  $T_{RD}$  ages indicate that many peridotites experienced Re depletion > 0.4  
660 Ga before formation of the Zealandia crust, which is Late Cambrian at its oldest but dominantly  
661 Mesozoic. Ages for duplicates are not included. Dominantly refractory classification refers to peridotite  
662 suites with olivine Mg# mostly > 91. The global abyssal trend represents the Os isotopic composition of  
663 the convecting mantle and is from Pearson et al. (2007), and the Kaapvaal Craton compilation example is  
664 from Pearson and Wittig (2008); note that the abyssal and Kaapvaal curves are relative probability  
665 distributions and do not correlate to the Y-axis (number of analyses for histogram).

666

667 **Figure 7.** Depletion indices versus platinum group elements. **7A.** Bulk rock Pd/Ir versus Al<sub>2</sub>O<sub>3</sub>. The most  
668 refractory samples, as judged by bulk rock Al<sub>2</sub>O<sub>3</sub> normalised to anhydrous conditions, generally  
669 correspond to lowest Pd/Ir. There is some evidence for P-PGE enrichment in the Pd/Ir > PUM, as is seen  
670 in most Dun Mountain Ophiolite and Auckland Island samples. **7B.** The lack of <sup>187</sup>Os/<sup>188</sup>Os linear arrays  
671 projected from PUM indicate that the Os isotopes record a history that involves decoupling of the PGE  
672 abundances from the Re-depletion events. Archean mantle Pd/Ir range is from Aulbach et al. (2016).

673

674 **Figure 8.** Formation of a modern continent. **8A.** Variably aged peridotitic material is brought into a  
675 subduction margin, amalgamated, and melted at low pressure (< 3 GPa) in the presence of water to  
676 generate refractory residues. Melting causes decoupling of Os isotopes from depletion indices. Some  
677 new domains undergo little or no re-melting and retain (or gain) moderately depleted compositions. The  
678 variably depleted peridotites are then progressively laterally accreted to the sub-arc lithosphere, which  
679 results in crust underpinned by autochthonous mantle. **8B.** Once subduction ceases, a buoyant platform  
680 comprising heterogeneous crust and variably depleted mantle lithosphere is formed. **8C.** If this  
681 lithosphere were thickened by compression, refractory portions of the root would chemically resemble  
682 Archean mantle lithosphere, as has occurred under the Southern Alps of New Zealand over the last ~7  
683 Ma. This figure also shows the distribution of terranes forming modern Zealandia (see also Fig. 2);  
684 DMOB, Dun Mountain Ophiolite Belt.



Figure 1  
[Click here to download high resolution image](#)

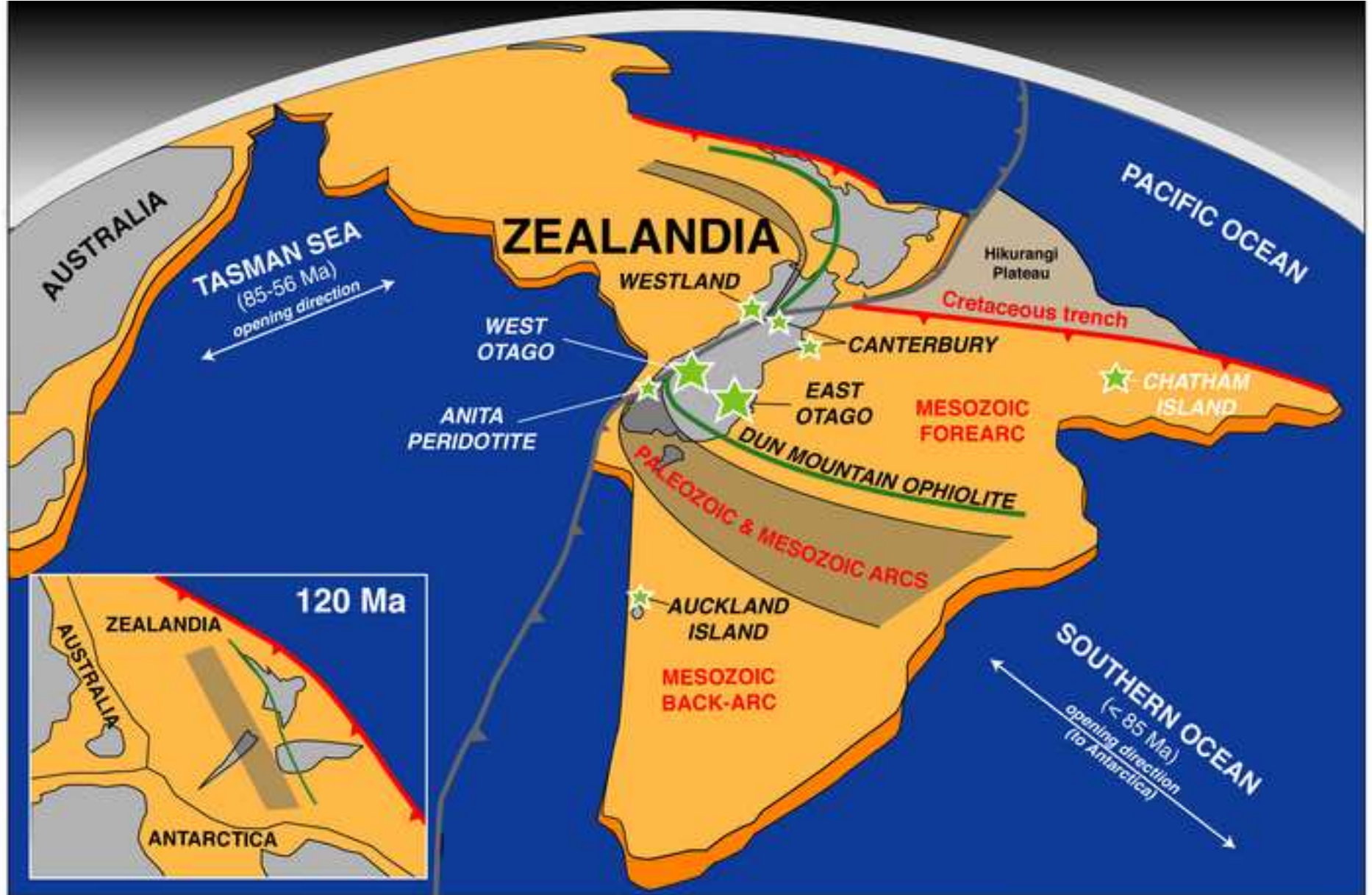


Figure 2  
[Click here to download high resolution image](#)

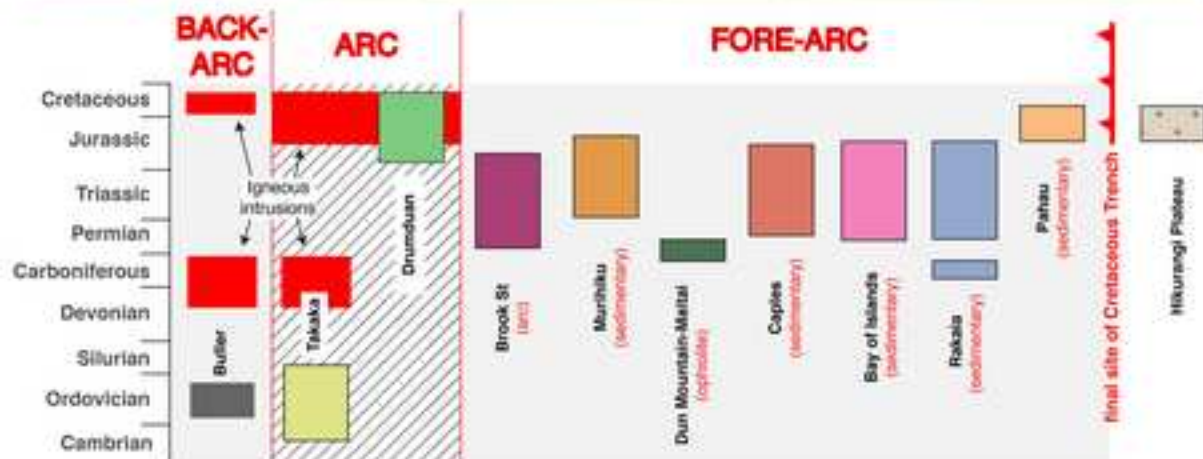
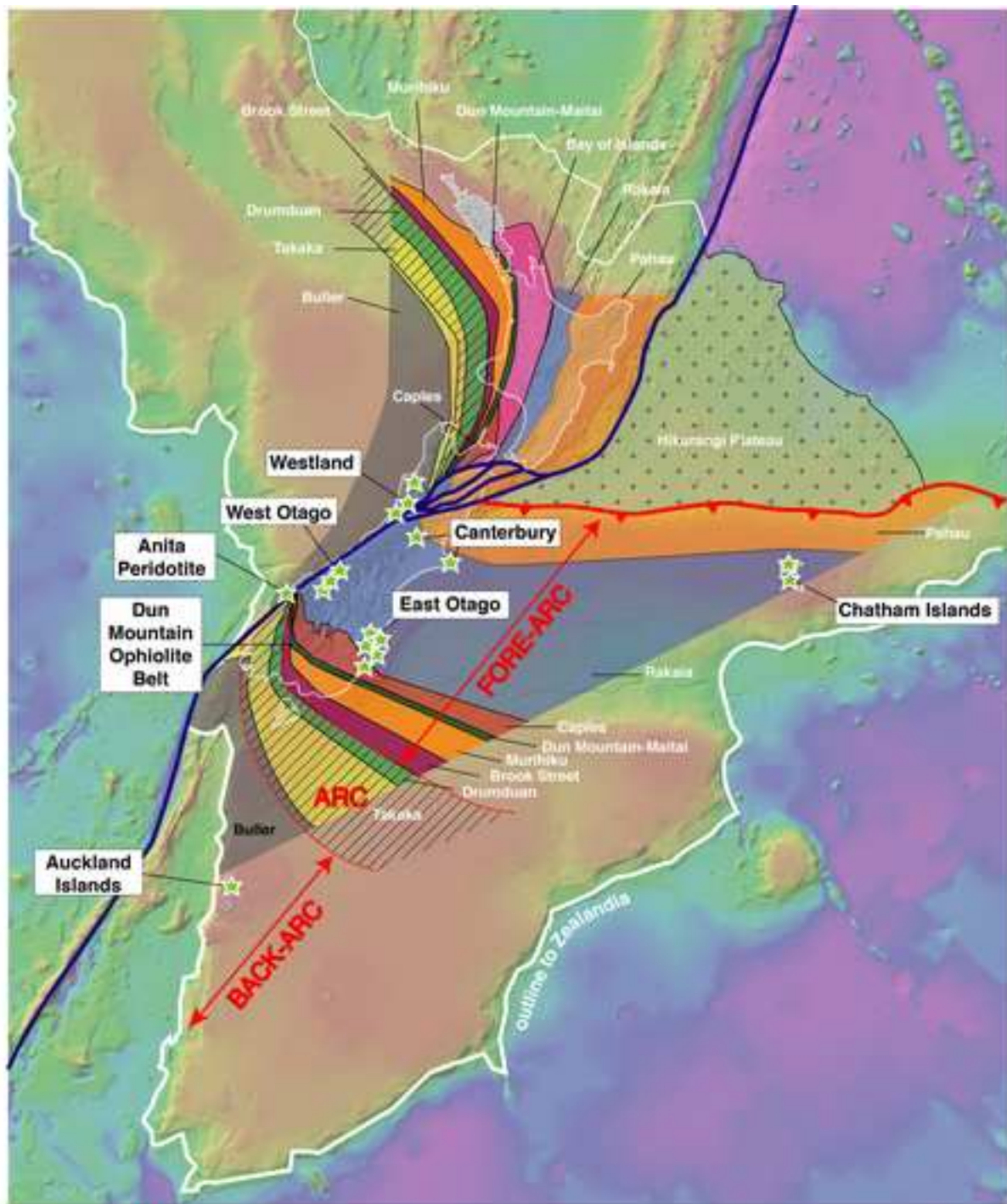


Figure 3  
[Click here to download high resolution image](#)

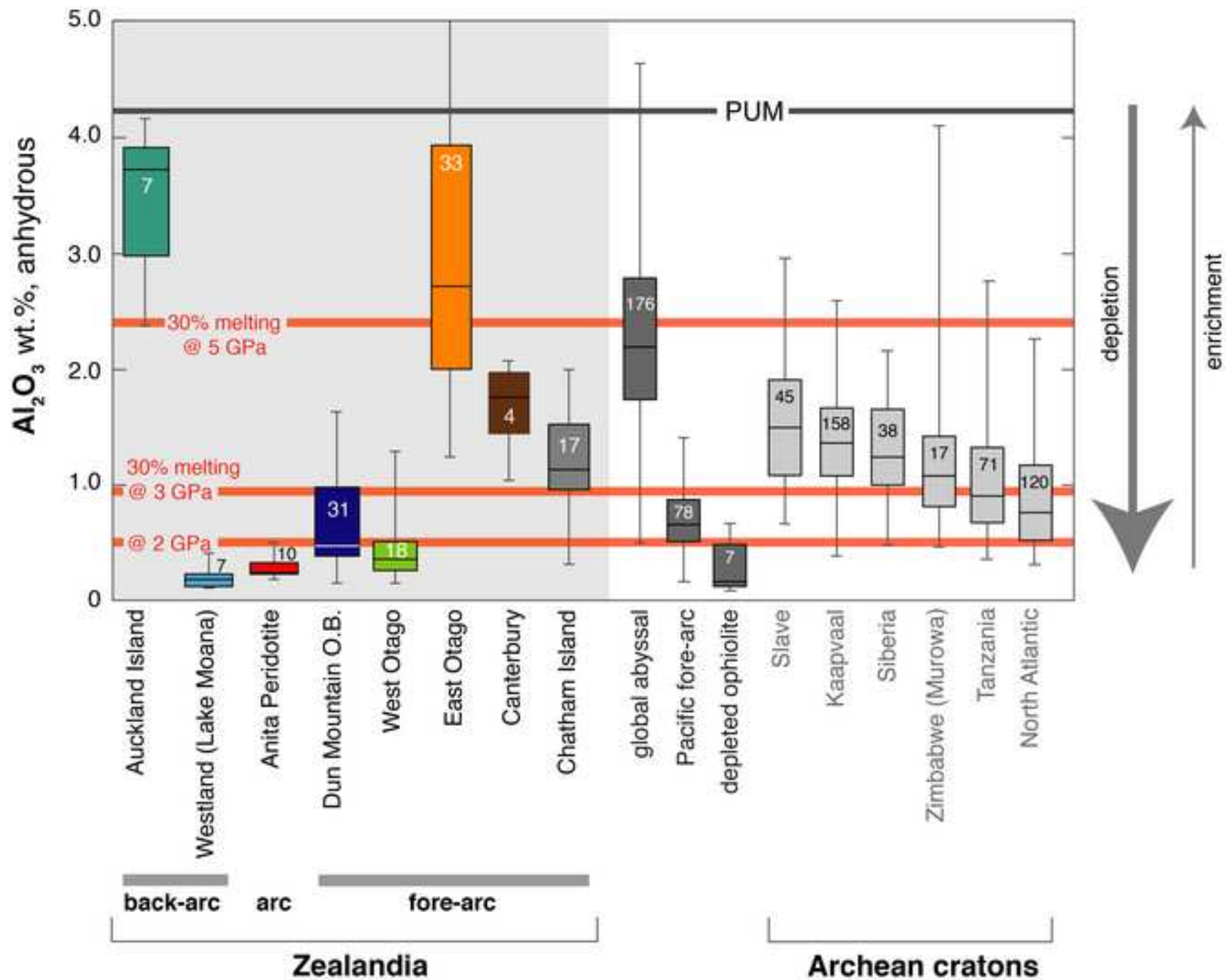


Figure 4

[Click here to download high resolution image](#)

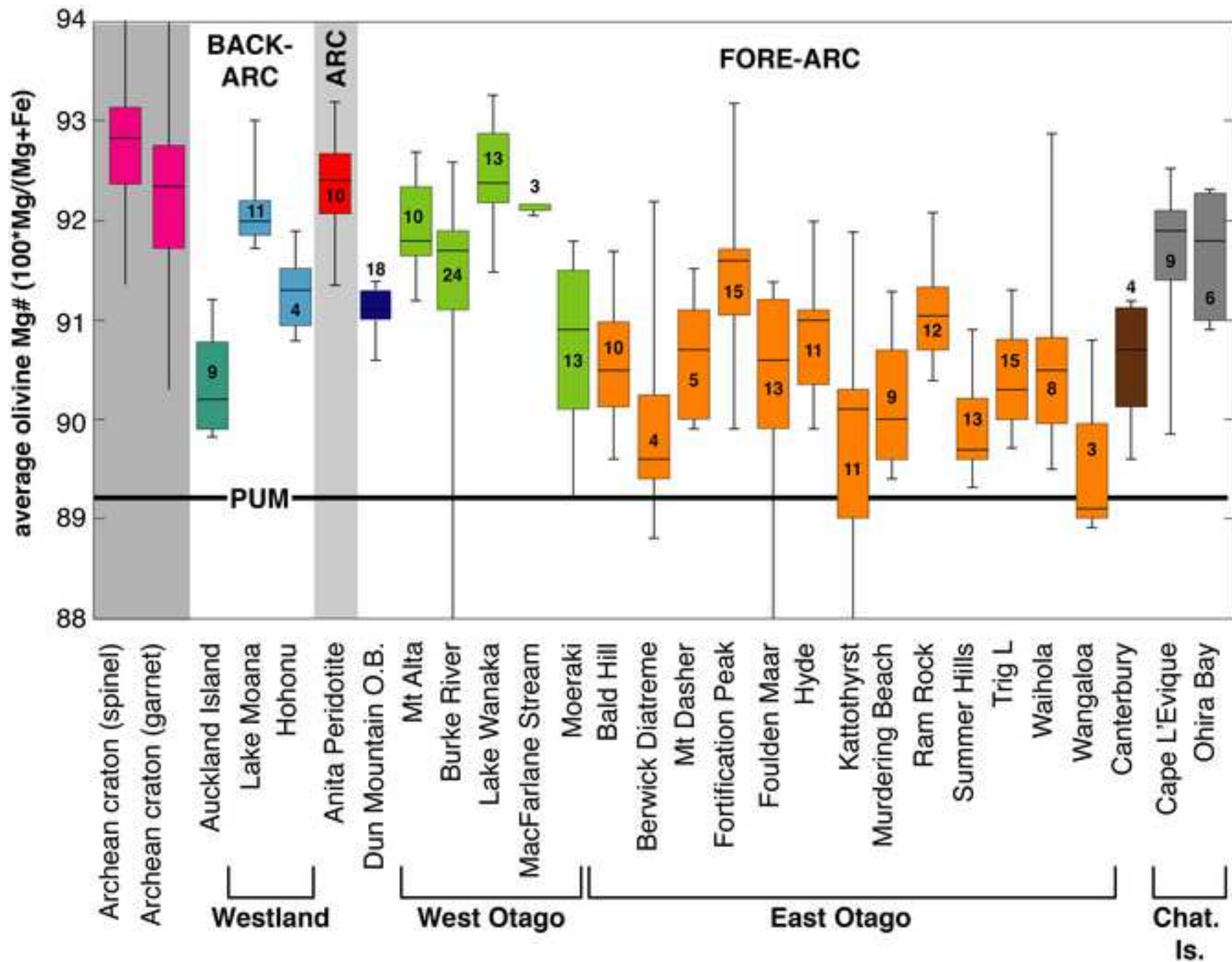


Figure 5  
[Click here to download high resolution image](#)

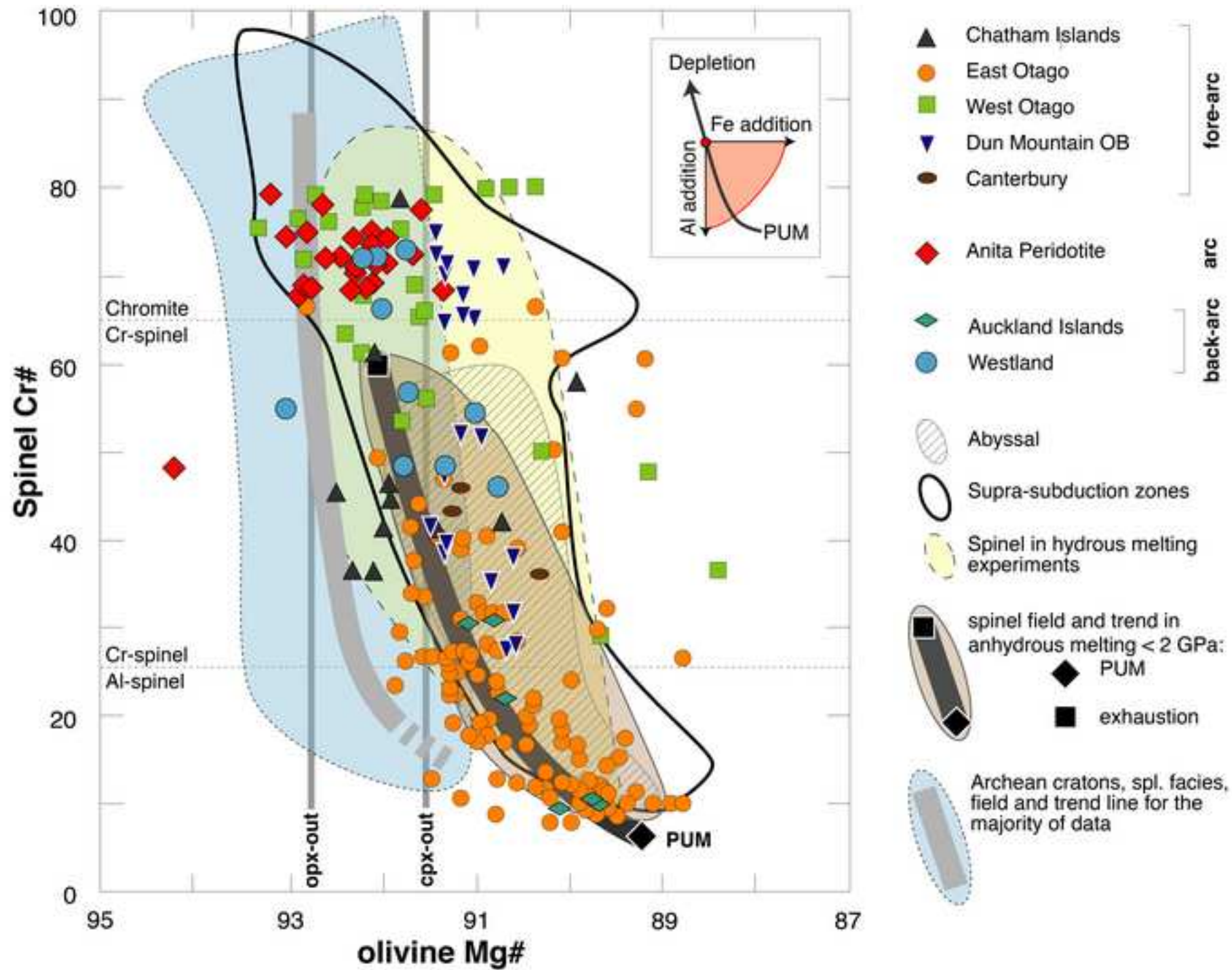




Figure 7  
[Click here to download high resolution image](#)

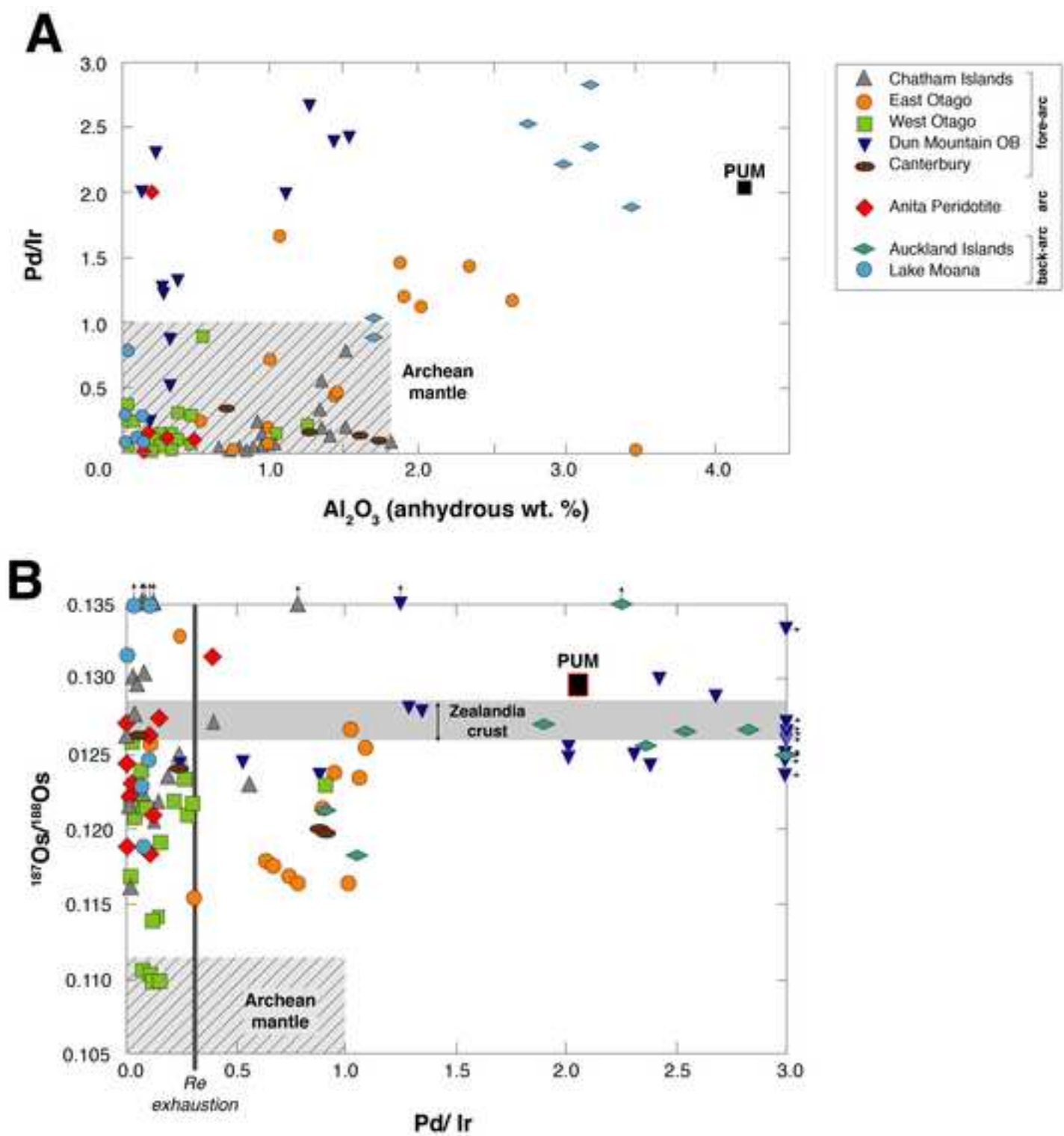


Figure 8  
[Click here to download high resolution image](#)

